Host-cell dependent role of phosphorylated keratin 8 during influenza A/NWS/33 virus (H1N1) infection in mammalian cells

Virus Research

Host-cell dependent role of phosphorylated keratin 8 during influenza A/NWS/33 virus (H1N1) infection in mammalian cells

--Manuscript Draft--

Manuscript Number:	VIRUS_2020_51R2
Article Type:	Research Paper
Keywords:	virus-host interaction; keratin 8; phosphorylation; intermediate filaments; Influenza A virus
Corresponding Author:	Flora De Conto, Assistant Professor Universita degli Studi di Parma Parma, ITALY
First Author:	Flora De Conto, Assistant Professor
Order of Authors:	Flora De Conto, Assistant Professor
	Francesca Conversano, Ph.D.
	Sergey Razin, Full Professor
	Silvana Belletti
	Maria Cristina Arcangeletti
	Carlo Chezzi
	Adriana Calderaro
Abstract:	In this study, we investigated the involvement of keratin 8 during human influenza A/NWS/33 virus (H1N1) infection in semi-permissive rhesus monkey-kidney (LLC-MK2) and permissive human type II alveolar epithelial (A549) cells. In A549 cells, keratin 8 showed major expression and phosphorylation levels. Influenza A/NWS/33 virus was able to subvert keratin 8 structural organization at late stages of infection in both cell models, promoting keratin 8 phosphorylation in A549 cells at early phases of infection. Accordingly, partial colocalizations of the viral nucleoprotein with keratin 8 and its phosphorylated form were assessed by confocal microscopy at early stages of infection in A549 cells. The employment of chemical activators of phosphorylation resulted in structural changes as well as increased phosphorylation of keratin 8 in both cell models, favoring the influenza A/NWS/33 virus's replicative efficiency in A549 but not in LLC-MK2 cells. In A549 and human larynx epidermoid carcinoma (HEp-2) cells inoculated with respiratory secretions from pediatric patients positive for, respectively, influenza A virus or respiratory syncytial virus, the keratin 8 phosphorylation level had increased only in the case of influenza A virus infection. The results obtained suggest that in A549 cells the influenza virus is able to induce keratin 8 phosphorylation thereby enhancing its replicative efficiency.
Suggested Reviewers:	Joanna Rzeszowska-Wolny joanna.rzeszowska@polsl.pl Her scientific interest concerns the information stored in living systems: regulation of the expression of genetic information, signal transduction, mechanisms induced by DNA damage and repair.
	Akira Ono akiraono@umich.edu His scientific interest is focused on mechanisms regulating assembly of viral components and effects of host factors
	simone giannecchini simone.giannecchini@unifi.it His scientific interest is focused on host cell-virus interaction
	Maria Antonia De Francesco maria.defrancesco@unibs.it Her scientific interest is focused on the molecular characterization of different viruses

Highlights

In A549 cells keratin 8 shows major expression and phosphorylation levels

Influenza A/NWS/33 virus promotes keratin 8 phosphorylation in A549 cells

Activators of phosphorylation favour the replication of influenza A/NWS/33 virus

Influenza A virus enhances its replication in A549 cells by phosphorylation

Figure 1

Click here to access/download;Figure;FIG1 .tif

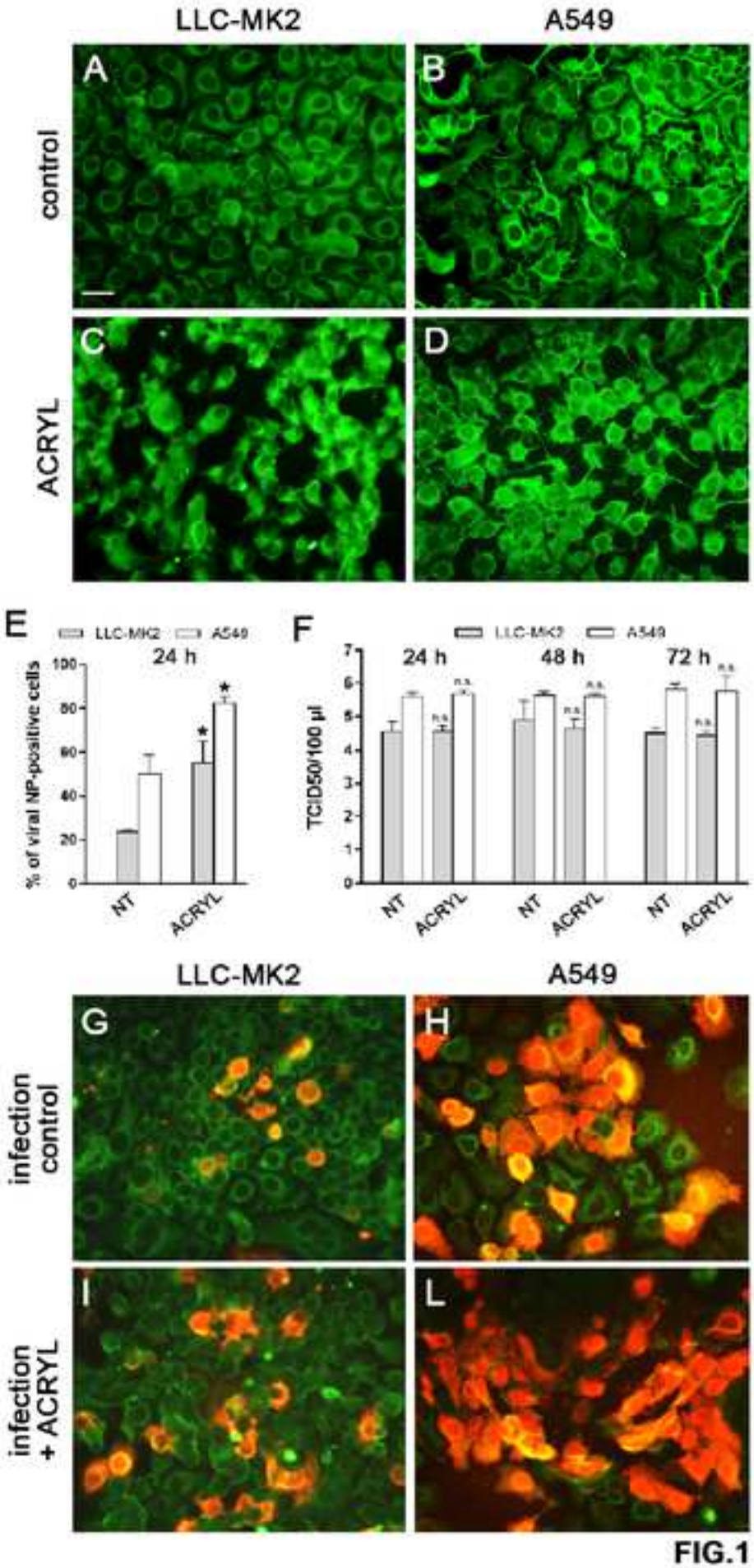

FIG.1

Figure 2

Click here to access/download;Figure;FIG2.tif

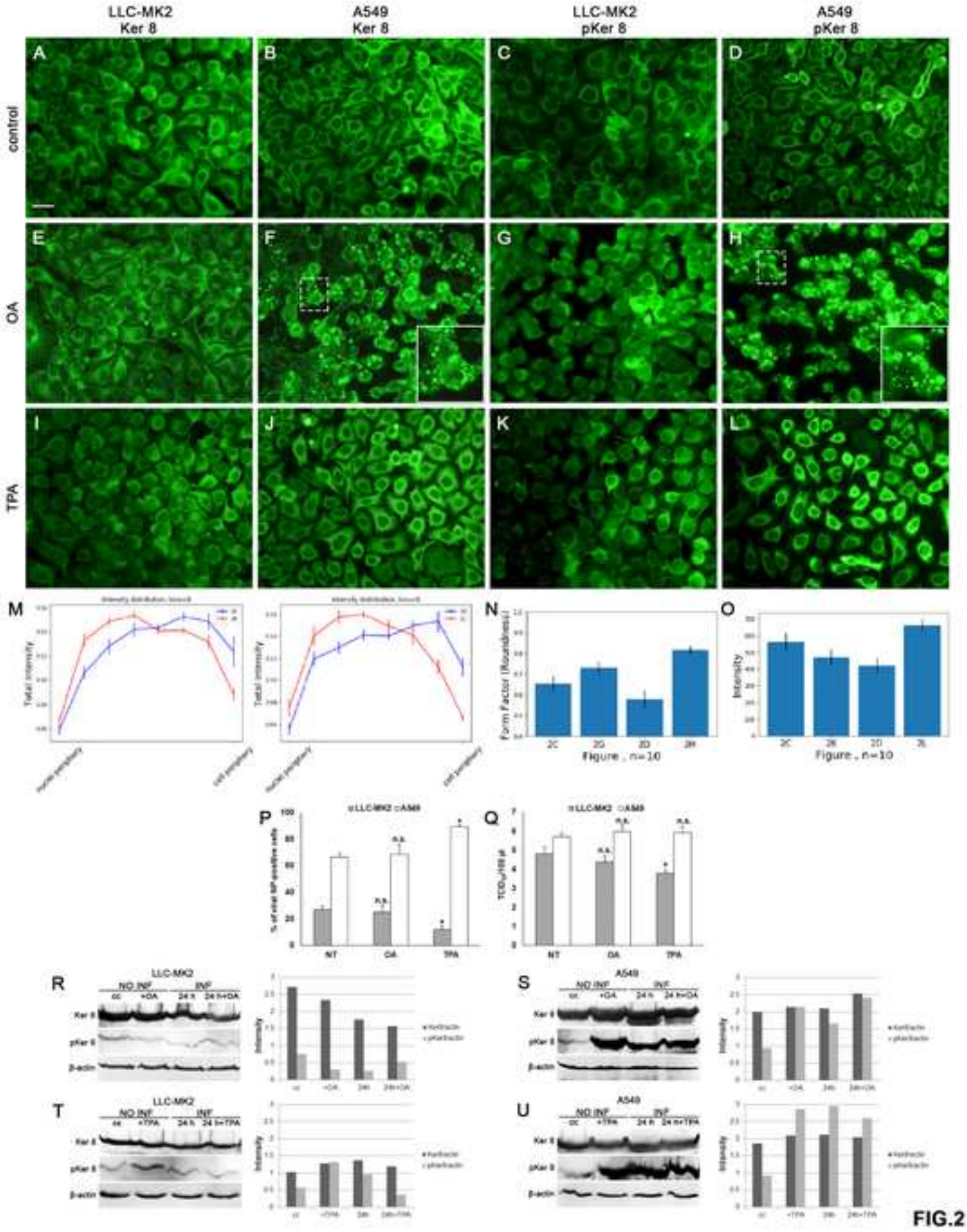

FIG.2

Figure 3

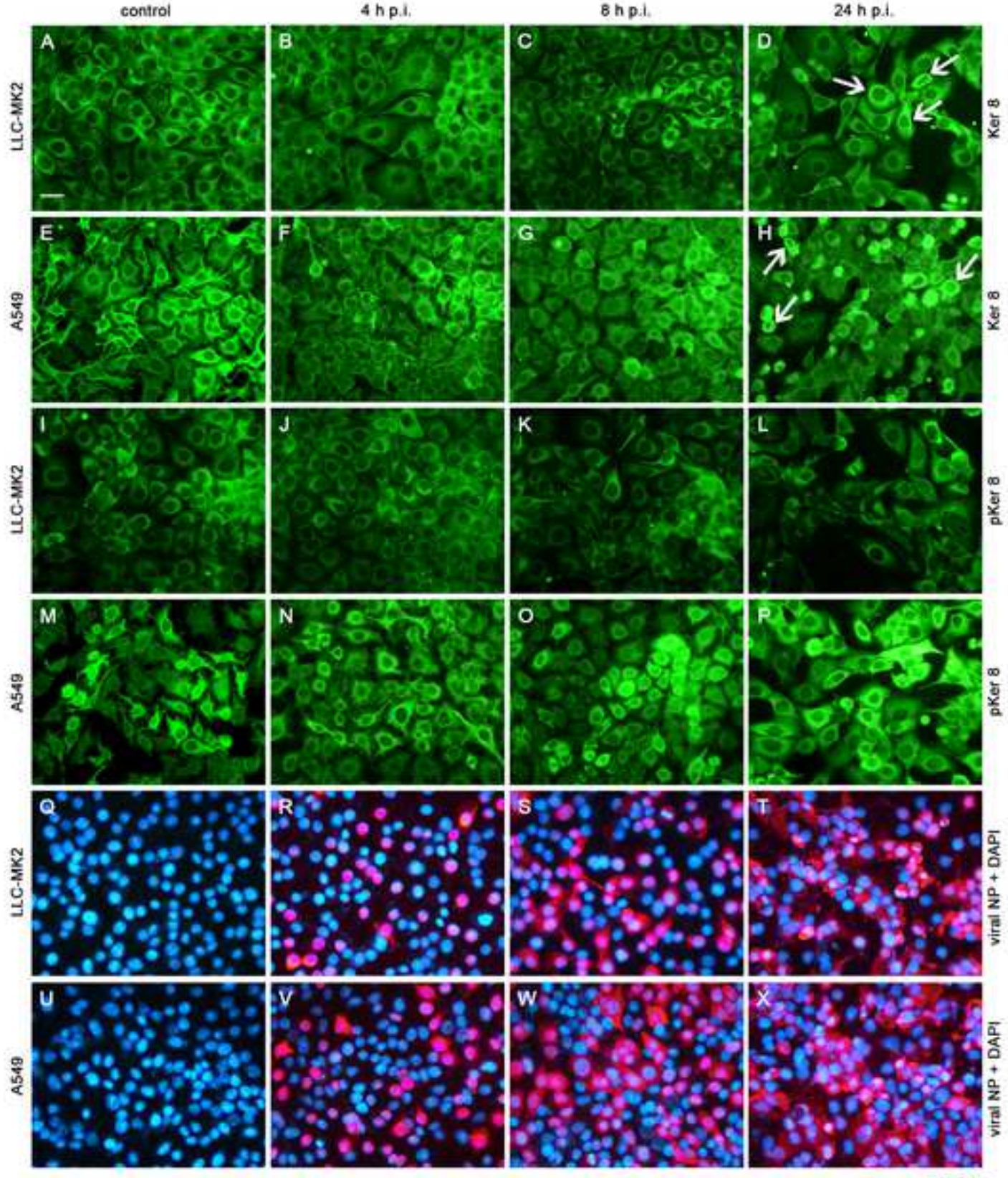

FIG.3

Figure 4

Click here to access/download;Figure;FIG4.tif

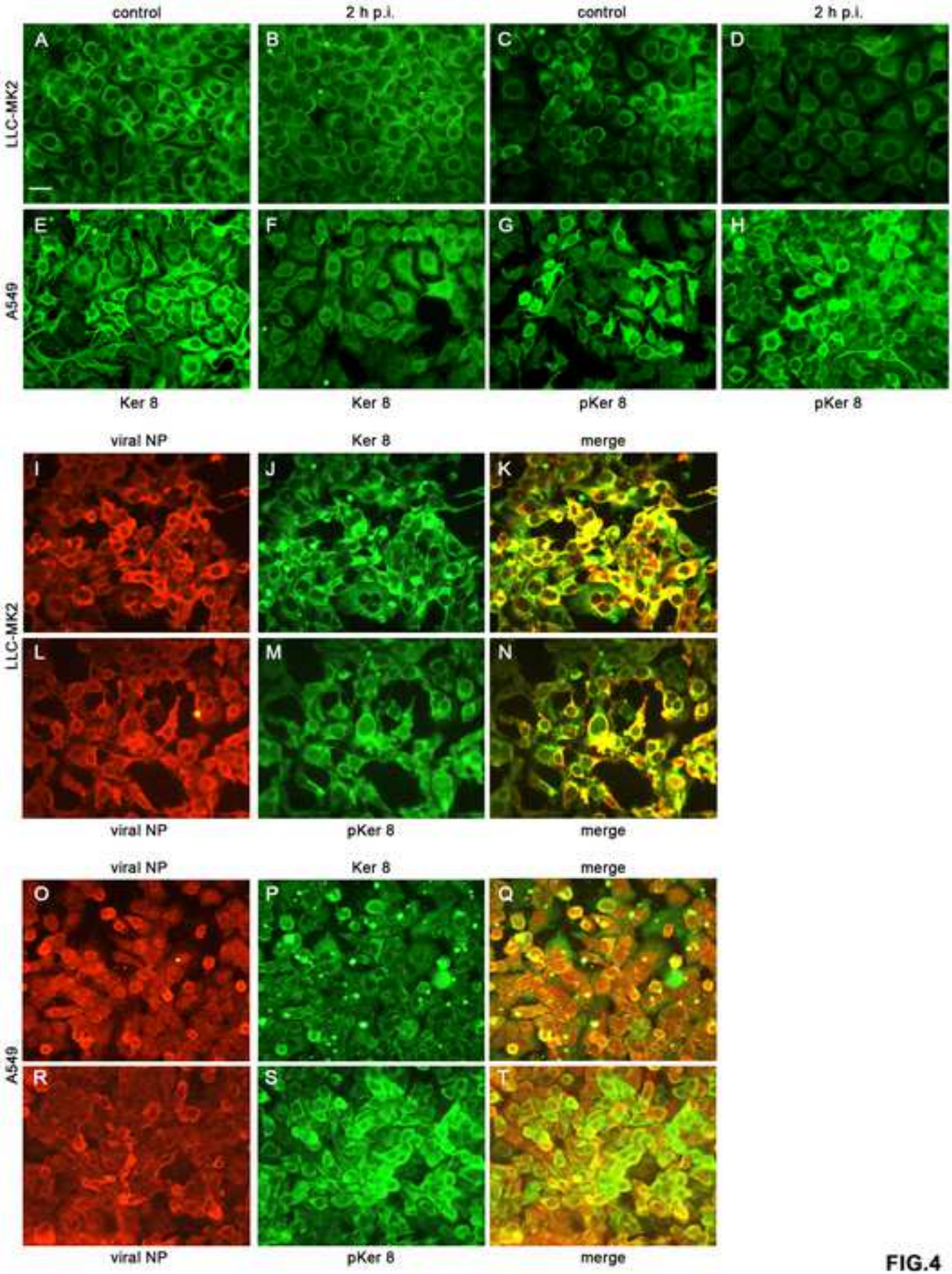

FIG.4

Figure 5

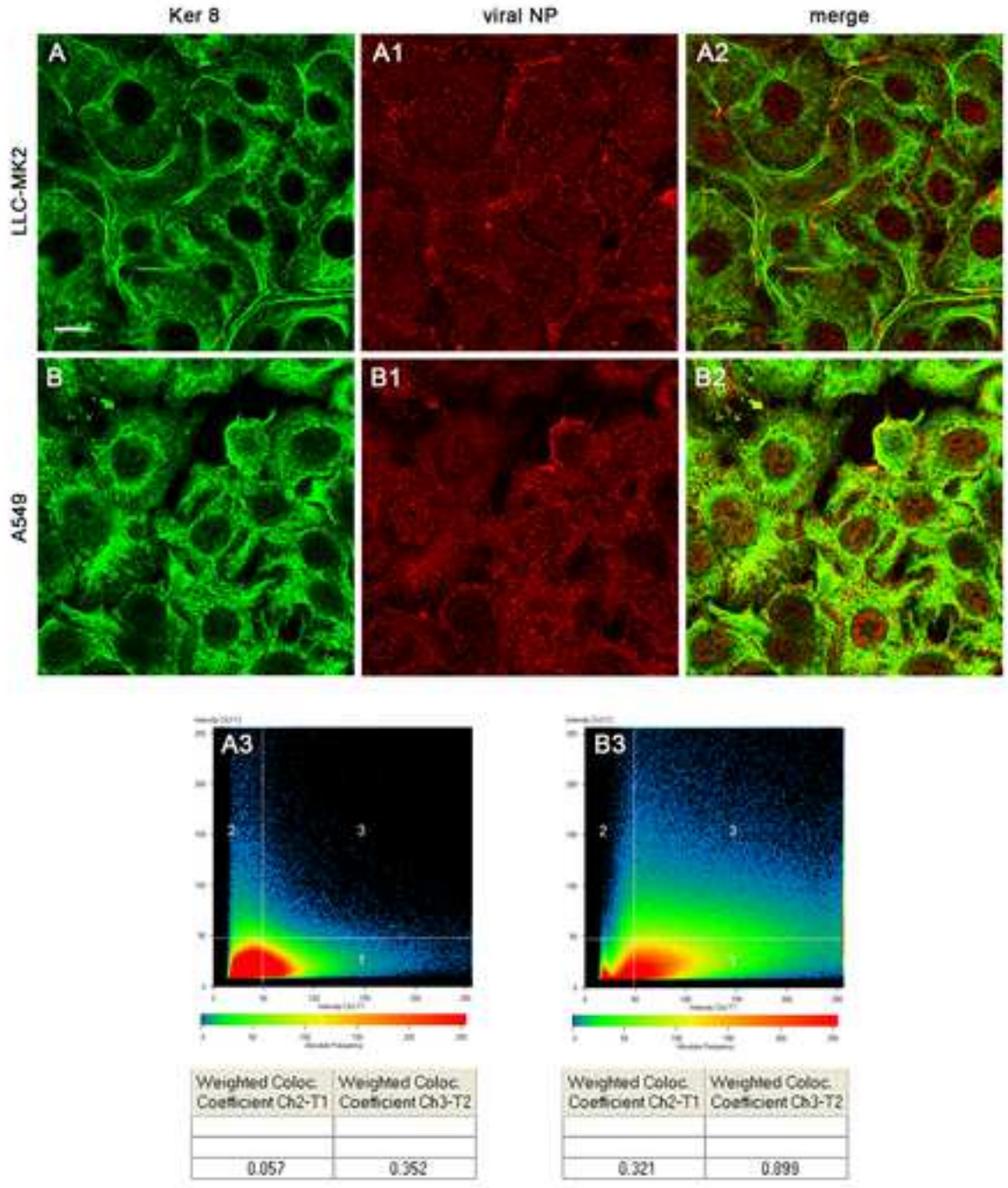

FIG.5

Figure 6

Click here to access/download;Figure;FIG6.tif

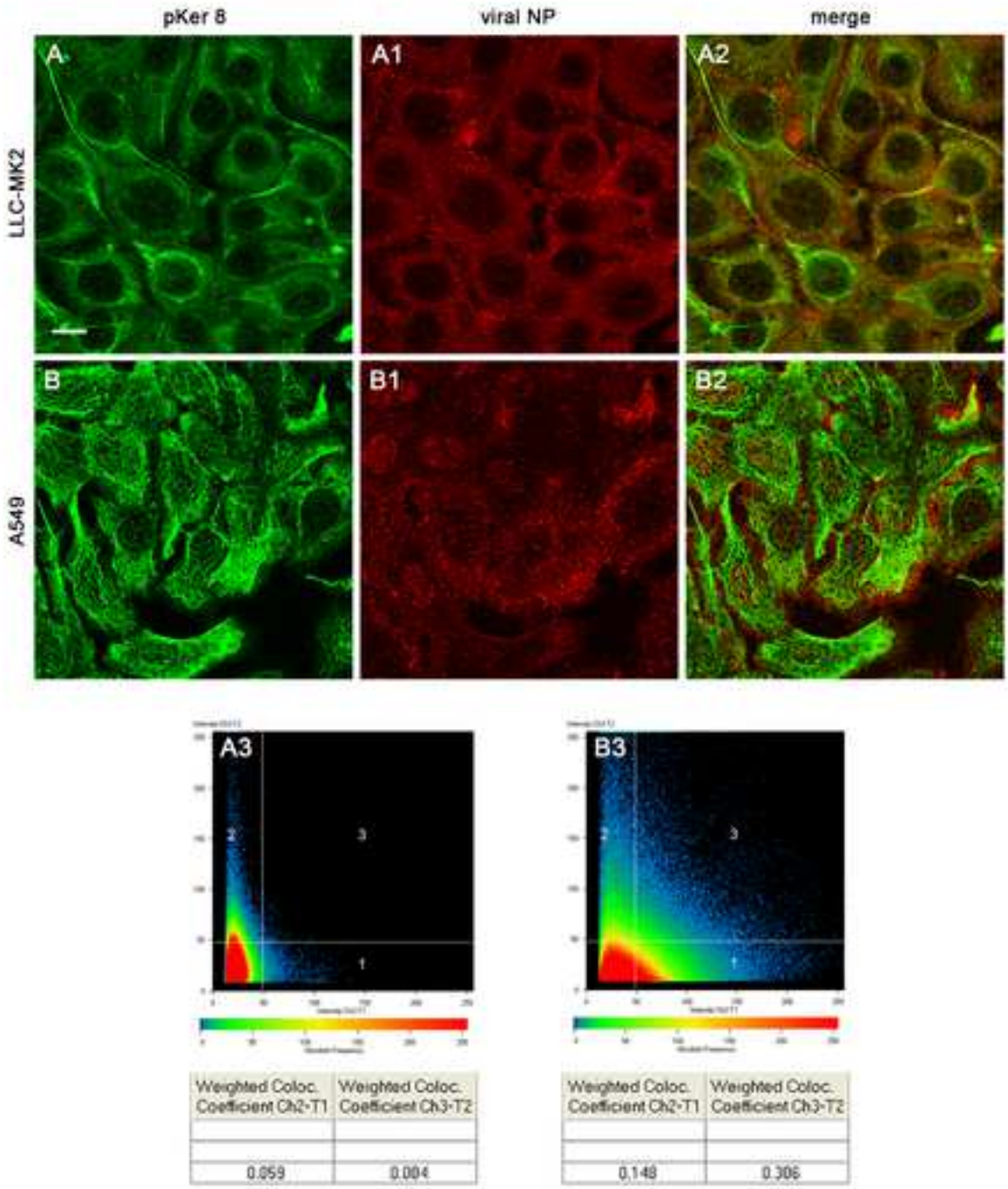

FIG.6

Figure 7

Click here to access/download;Figure;FIG7.tif

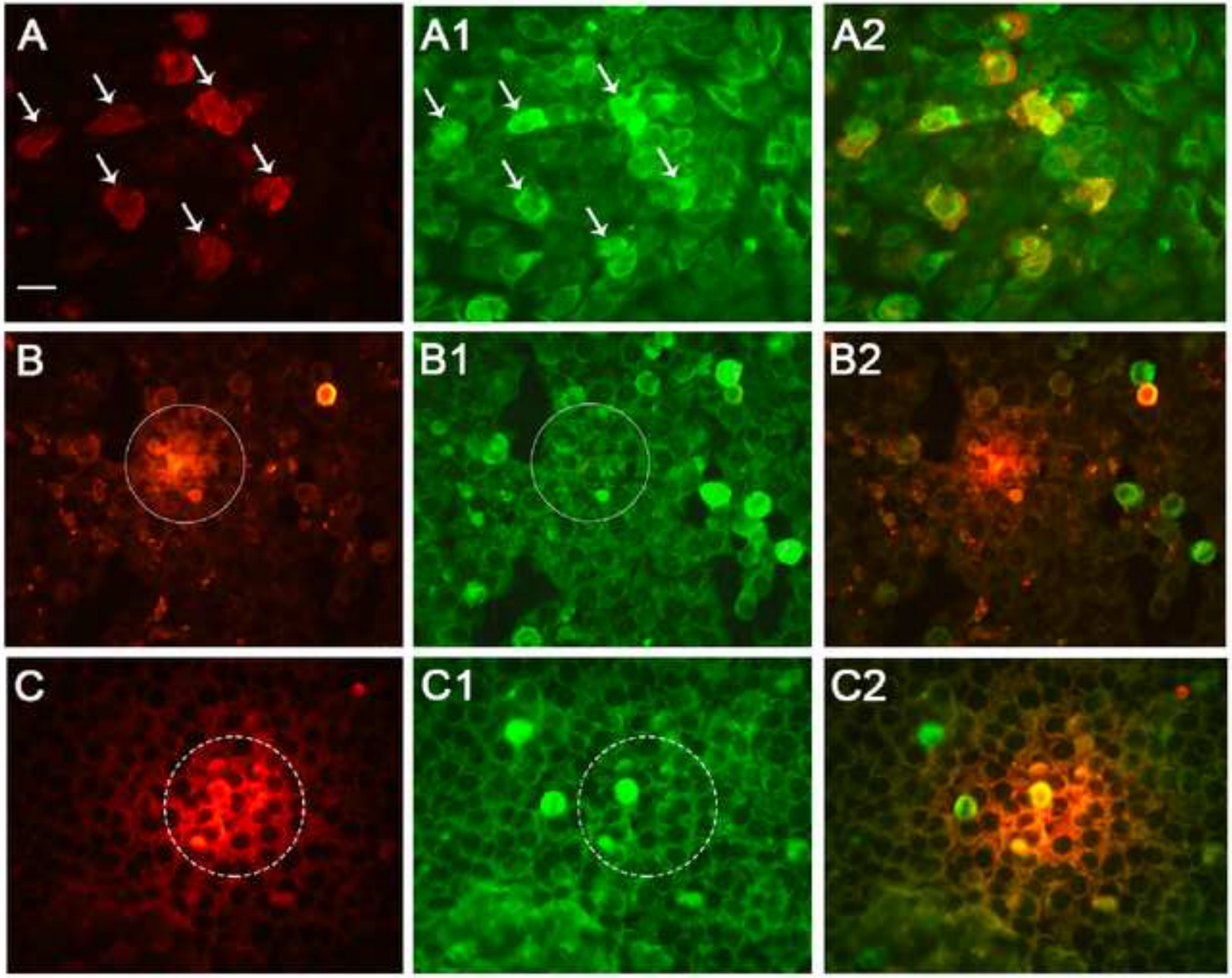

FIG.7

CREDIT AUTHOR STATEMENT

Flora De Conto: conceptualization, validation, investigation, funding acquisition, writing original draft, writing review and editing, resources; **Francesca Conversano**: investigation, writing original draft, visualization; **Sergey V. Razin**: investigation, writing review and editing; **Silvana Belletti**: investigation, visualization; **Maria Cristina Arcangeletti**: investigation, data curation; **Carlo Chezzi**: writing review and editing, supervision, validation; **Adriana Calderaro**: writing review and editing, supervision, validation.

Supplementary Figure 1

Supplementary Figure 2

Host-cell dependent role of phosphorylated keratin 8 during influenza A/NWS/33 virus (H1N1) infection in mammalian cells

Flora De Conto*[1], Francesca Conversano[1], Sergey V. Razin[2], Silvana Belletti[1], Maria Cristina Arcangeletti[1], Carlo Chezzi[1], Adriana Calderaro[1]

[1] Department of Medicine and Surgery, University of Parma, Parma, Italy

[2] Institute of Gene Biology, Russian Academy of Sciences and Lomonosov Moscow State University, Moscow, Russia

* Author for correspondence: Flora De Conto

Department of Medicine and Surgery, University of Parma, Viale A. Gramsci 14, 43126 Parma, Italy.

E-mail: flora.deconto@unipr.it phone: +39 0521 033496 fax: +39 0521 993620

ABSTRACT

In this study, we investigated the involvement of keratin 8 during human influenza A/NWS/33 virus (H1N1) infection in semi-permissive rhesus monkey-kidney (LLC-MK2) and permissive human type II alveolar epithelial (A549) cells. In A549 cells, keratin 8 showed major expression and phosphorylation levels. Influenza A/NWS/33 virus was able to subvert keratin 8 structural organization at late stages of infection in both cell models, promoting keratin 8 phosphorylation in A549 cells at early phases of infection. Accordingly, partial colocalizations of the viral nucleoprotein with keratin 8 and its phosphorylated form were assessed by confocal microscopy at early stages of infection in A549 cells. The employment of chemical activators of phosphorylation resulted in structural changes as well as increased phosphorylation of keratin 8 in both cell models, favoring the influenza A/NWS/33 virus's replicative efficiency in A549 but not in LLC-MK2 cells. In A549 and human larynx epidermoid carcinoma (HEp-2) cells inoculated with respiratory secretions from pediatric patients positive for, respectively, influenza A virus or respiratory syncytial virus, the keratin 8 phosphorylation level had increased only in the case of influenza A virus infection. The results obtained suggest that in A549 cells the influenza virus is able to induce keratin 8 phosphorylation thereby enhancing its replicative efficiency.

Keywords: virus-host interaction; keratin 8; phosphorylation; intermediate filaments; Influenza A virus.

Abbreviations: A549 – human type II alveolar epithelial; ACRYL – acrylamide; BSA – bovine serum albumin; DAPI – 4',6-diamidino-2-phenylindole dihydrochloride; IF – intermediate filament; IIF – indirect immunofluorescence; HEp-2 human larynx epidermoid carcinoma; Ker 8 – keratin 8; LLC-MK2 – rhesus monkey-kidney; MDCK – Madin-Darby canine-kidney; MOI – multiplicity of infection; NP –nucleoprotein; n.s. – not statistically significant; NWS/33 virus – human influenza A/NWS/33 virus; OA – okadaic acid; PBS – phosphate-buffered saline; PFU – plaque forming units; p.i. – post-infection; pKer 8 – phosphorylated keratin 8 on serine 432; PKC – protein kinase C; PTM – post-translational modification; RSV – respiratory syncytial virus; $TCID_{50}$ – fifty % tissue culture infectious dose; TPA – 12-O-tetradecanoylphorbol-13-acetate; WB – Western blotting.

1. Introduction

Influenza viruses depend on specific cellular components/functions to perform their replication. A widespread understanding of the influenza virus-host cell interface could highlight suitable targets for innovative antiviral drugs, improving the treatment and prevention of influenza.

Concerning the involvement of the cell cytoskeleton, we previously demonstrated that stable microfilaments and microtubules constitute a restriction factor for human influenza A/NWS/33 virus (NWS/33 virus) infection (Arcangeletti et al., 2008; De Conto et al., 2018, 2015, 2012, 2011). Importantly, although previous studies mainly described the regulatory role of intermediate filaments (IFs) during virus infection through chemical perturbation or small interfering RNA (siRNA)-mediated depletion of specific IFs components (Arcangeletti et al., 1997; Hertel, 2011; Matsuda et al., 2005; Miller and Hertel, 2009; Shoeman et al., 2001; Sripada and Dayaraj, 2010; Wu and Pantè, 2016), the knowledge about the involvement of the IFs post-translational modifications remains limited (Stefanovic et al., 2005; Chiou et al., 2012; McIntosh et al., 2010).

IFs are formed by members of a very large family of cell-specific proteins sharing both sequence homology and structural features (Busch et al., 2012). Among IF proteins, keratins are the most abundantly expressed in epithelial cells (Hyder et al., 2008). IF proteins are regulated by several post-translational modifications (PTMs), which mainly appear under specific conditions, such as stress-response, cell migration, mitosis, and apoptosis (Hyder et al., 2008; Omary et al., 2006; Sawant and Leube, 2017; Snider and Omary, 2016). Among the PTMs, phosphorylation has been found to be involved in the control of the assembly/disassembly of IFs (Hyder et al., 2008; Izawa and Inagaki, 2006; Omary et al., 2006; Sihag et al., 2007). Specifically, keratin 8 (Ker 8) phosphorylation induces the reorganization of keratin filaments, promoting the migration of epithelial tumor cells (Busch et al., 2012) and modulating the stretch response of keratin in epithelial cells (Fois et al., 2013).

This study aimed to investigate the role of Ker 8 and its phosphorylated state during NWS/33 virus infection in LLC-MK2 and A549 mammalian cells, showing differing levels of permissiveness. To this aim, experiments were carried out by using chemical treatments able to modulate the structural organization and phosphorylation level of Ker 8.

Here we describe that Ker 8 phosphorylation modulates virus infection in a virus- and cell-dependent way. More specifically, Ker 8 phosphorylation augmented in A549 but not in LLC-MK2 cells during influenza A virus infection, favoring the virus replication cycle. Conversely, the parallel analysis of respiratory syncytial virus (RSV) infection in HEp-2 cells assessed unchanged levels of Ker 8 phosphorylation.

2. Materials and methods

2.1. Cell lines

A549 (TCL 101), LLC-MK2 (BS CL 57), HEp-2 (BS TCL 23), and Madin-Darby canine-kidney (MDCK, BS CL 64) cells were from the Lombardy and Emilia Romagna Experimental Zootechnic Institute (*IZSLER*) (Brescia, Italy). Cells were cultured in Ham's F-12 Nutrient Mixture (A549) and Earle's Modified Eagle's Medium (LLC-MK2, HEp-2, and MDCK), containing 2 mM L-glutamine, 10% fetal bovine serum and antibiotics (100 U/ml penicillin and 100 µg/ml streptomycin). Cells were kept at 37°C in a humidified atmosphere with 5% CO_2. Culture reagents were from EuroClone.

2.2. Viral infection

Human influenza A/NWS/33 virus (H1N1; ATCC VR 219) was propagated as previously detailed (Arcangeletti et al., 2008). LLC-MK2 and A549 cells grown to confluence in shell-vials or 6-well plates were infected at a multiplicity of infection (MOI) of 0.1, 2, and 10 plaque-forming units (PFU)/cell to either better evidence the host cell-dependent susceptibility to virus infection or better visualize the virus staining by confocal microscopy analyses. After adsorption for 75 min at 4°C, the viral inoculum was removed, and cells were washed twice with serum-free Earle's Modified Eagle's Medium, before incubation for the time indicated.

2.3. Infection of A549 and HEp-2 cells with respiratory samples from patients with acute respiratory disease

A total of 10 nasal and throat swabs from pediatric patients with acute respiratory disease observed at the University Hospital of Parma (Northern Italy) were stored at 4°C in viral transport medium until submitted to the Unit of Virology. Laboratory diagnosis of respiratory infections was performed upon medical request. The patients' identity and medical information were rigorously protected and remained anonymous throughout the study. Upon rapid culture method carried out as previously described (De Conto et al., 2019), the samples found positive for either influenza A virus (5 samples) or RSV (5 samples), were, respectively, inoculated in A549 and HEp-2 cell monolayers. At 24 or 48 h post-infection (p.i.), IIF analysis of phosphorylated Ker 8 on serine 432 (pKer 8) together with influenza A virus nucleoprotein (NP) and RSV fusion protein was carried out.

2.4. Antibodies

For IIF assays, mouse monoclonal anti-influenza A virus NP (1:30; Argene/BioMérieux) and anti-RSV fusion protein (1:30; Argene/BioMérieux) antibodies were used. Additionally, rabbit polyclonal anti-Ker 8 (1:100; Thermo Fisher Scientific) and anti-pKer 8 (1:100; Thermo Fisher Scientific) antibodies were employed. Bound antibodies were detected by Alexa Fluor 568 goat anti-mouse IgG (1:470; Molecular Probes) and fluorescein isothiocyanate-conjugated donkey anti-rabbit IgG (1:70; Li StarFish) antibodies. Lastly, 4',6-diamidino-2-phenylindole dihydrochloride (DAPI; 2.5 µg/ml; Sigma-Aldrich) was employed during the IIF assays to detect nuclear chromatin.

For Western blotting (WB) assays, mouse monoclonal anti-beta-actin IgG (1:400; Santa Cruz Biotechnology), rabbit polyclonal anti-Ker 8 (1:3,000; Thermo Fisher Scientific), and anti-pKer 8 (1:500; Thermo Fisher Scientific) antibodies were employed. Bound antibodies were detected by anti-mouse (1:5,000; Sigma-Aldrich) and anti-rabbit (1:5,000; Sigma-Aldrich) IgG alkaline phosphatase-conjugated antibodies.

2.5. Drug treatment

Cells grown in shell-vials or 6-well plates were treated with different chemical modulators of IFs. Depolymerization of the IFs was obtained using acrylamide (ACRYL; 5 mM) treatment. To induce Ker 8 phosphorylation, the cells were treated with either phosphatase inhibitor okadaic acid (OA; 0.05 µg/ml) or protein kinase C (PKC) activator 12-O-tetradecanoylphorbol-13-acetate (TPA; LLC-MK2: 25 nM; A549: 50 nM). ACRYL was from Bio-Rad, while OA and TPA were from Sigma-Aldrich.

2.6. Indirect immunofluorescence assay

After performing the experimental infection and/or drug treatments, LLC-MK2 and A549 cell monolayers were fixed and permeabilized in methanol for 5 min at -20°C. The cells were then washed with phosphate-buffered saline (PBS, pH 7.4; 7 mM Na_2HPO_4, 1.5 mM KH_2PO_4, 137 mM NaCl, 2.7 mM KCl), blocked with 1% bovine serum albumin (BSA; PAA Laboratories GmbH) in PBS, and incubated with primary antibodies diluted in 0.2% BSA in PBS for 1 h at 37°C. After washes with PBS, the cells were incubated with the secondary antibodies diluted in 0.2% BSA in PBS for 45 min at 37°C. For negative controls, the primary antibodies were replaced by 0.2% BSA in PBS. The cells were mounted in buffered glycerol solution

(Argene/BioMérieux) and analyzed through an epifluorescence microscope (DMLB Leica). For each cell monolayer, ten randomly selected microscopic fields were acquired using a DC 300F camera (Leica) and then the most representative images were selected. For viral NP fluorescence quantization, ten randomly selected fields per cell monolayer were analyzed, and viral NP-positive cells expressed as mean percentage values of the total cell number per field, estimated by chromatin staining with DAPI. IIF assays were performed twice in two replicate shell-vials for each experimental condition.

2.7. Fifty percent tissue culture infectious dose ($TCID_{50}$) assay

Viral yields from culture supernatants were assessed in MDCK cells using a $TCID_{50}$ assay, as previously described (De Conto et al., 2012).

2.8. Western blotting assay

Cell lysates were collected as previously described (Arcangeletti et al., 2008). Briefly, aliquots containing 30 µg of proteins were loaded onto sodium dodecyl sulphate-13% polyacrylamide gel electrophoresis. The resolved proteins were transferred onto nitrocellulose blotting membranes (Bio-Rad). Subsequently, WB assays were performed according to the experimental protocol previously described (De Conto et al., 2018) and carried out twice with cell lysates collected from two replicate wells for each experimental condition.

For the assay of phosphorylation specificity, the nitrocellulose blotting membrane was first incubated for 30 min in phosphatase buffer (0.2 mM EDTA, 0.1 M TrisHCl, pH = 8.5) in the presence or absence of alkaline phosphatase from calf intestine (20 units/ml, ThermoFisher Scientific), according to Maya and Oren (2000). The membrane was then rinsed twice in distilled water, before the WB assay.

2.9. Confocal microscopy

Confocal microscopy was carried out as previously described (De Conto et al., 2018), using a Zeiss LSM 510 Meta inverted confocal microscope with a 63 x 1.4 NA oil immersion objective. For analysis of colocalization, a scatter diagram of the number of red pixels against the number of green pixels was generated from each merged image. Negative controls were examined in parallel to assess the specificity of the signals and absence of any background. No mutual cross talking of the red and green signals was detectable. The weighted

colocalization coefficients represent the sum of intensity of colocalizing pixels in red and green channels, as compared to the overall sum of pixel intensity above threshold. The weighted coefficient could be 0 (no colocalization) or 1 (all pixels colocalized). Bright pixels contributed more signal than faint pixels. Profile display mode was used for the intensity profile graphs.

2.10. Trypan blue exclusion assay

To determine the cell vitality, the trypan blue exclusion assay was carried out accordingly to Strober (2015). Briefly, the cells grown in 6-well plates were first subjected to different chemical treatments and then trypsinized. The cells were collected in PBS, before centrifugation at 2,500 x *g* for 5 min. The cell pellet was resuspended in 0.5 ml of PBS, before addition of 0.5 ml of 0.4% trypan blue in PBS (1:1 dilution). The mixture was incubated for 3 min at room temperature. The viable cells were counted within 5 minutes with a Burker counting chamber through the exclusion of trypan blue.

2.11. Quantitative image analysis

Cells images were analyzed using the CellProfiler software (version 3.1.5). Boundary of 10 cells per experiment were manually identified and nuclei region was excluded. To analyze distribution of intensity of immunostaining of proteins, each cell was divided onto 8 equal size shells. For each shell, the fraction of total staining (FractAtD) was calculated. To analyze the overall intensity of immunostaining an Integrated Intensity parameter was calculated for each cell.

Western blot images were analyzed by using the Fiji software (version 2.0.0-rc69/1.52p).

2.12. Statistical analysis

Statistical analysis was performed using GraphPad Prism software. A two-tailed Student's t-test was used to analyze differences between untreated and drug-treated as well as uninfected and infected LLC-MK2 and A549 cells. P values < 0.05 were considered statistically significant.

3. RESULTS

3.1. Depolymerization of IFs modulates influenza A/NWS/33 virus replication in LLC-MK2 and A549 cells

In the first set of experiments, we analyzed the effects of IF depolymerization on influenza virus infection in LLC-MK2 and A549 cells. Preliminary experiments (data not shown) were carried out to assess the concentration and the minimum treatment-time with ACRYL (*i.e*. 4 h) able to induce well discernible IFs depolymerization. Then the ACRYL treatment was maintained twice as long (*i.e*. 8 h), verifying that no further morphological changes of IFs as well as toxic effects occurred (Supplementary Table 1).

The cells either left untreated or treated with ACRYL for 8 h, were subjected to IIF analysis to detect Ker 8 (Figs. 1A-D). The results in untreated cells showed the radial distribution of Ker 8 filaments from the perinuclear region to the cell periphery, with a more pronounced network of filaments in A549 cells (Fig. 1B vs. 1A). Treatment with ACRYL stimulated the depolymerization of Ker 8 in both models, with more overt outcomes in LLC-MK2 cells (Fig. 1C vs. 1D).

Then, cells which were either left untreated or pre-treated for 4 h with ACRYL to induce IFs depolymerization were infected with NWS/33 virus (MOI = 0.1 PFU/cell, 24 h) in the absence or presence of the drug for 4 h p.i. for a total 8 h treatment-time (Figs. 1E and 1G-L). The cells were then subjected to double IIF staining to detect viral NP in comparison with Ker 8 (Figs. 1E, and 1G-L). The infection rate was monitored by evaluating viral NP-positive cells (Fig. 1E). The results showed that the depolymerization of the IFs had caused an increase in the portion of viral NP-positive cells in both cell models (Fig. 1E; Fig. 1I vs. 1G, and Fig. 1L vs. 1H).

Next, we checked using a $TCID_{50}$ assay whether the above-mentioned drug treatment had interfered with emergence of the viral progeny (Fig. 1F). Surprisingly, the titers of infectious viruses assessed in culture supernatants of LLC-MK2 and A549 cells treated with ACRYL at 24 h p.i., as described above, were similar to those of supernatants from untreated cells. Therefore, additional experiments were carried out in order to determine if longer times of virus infection (i.e. 48 and 72 h p.i.) at the above-described experimental conditions would have allowed the emergence of greater viral yields. The results assessed almost univariate viral yields over several infectious cycles (Fig. 1F).

3.2. Chemical activation of Ker 8 phosphorylation favors influenza A/NWS/33 virus infection in A549 cells

Considering the fact that depolymerization of Ker 8 may well be stimulated by Ker 8 phosphorylation (Moch et al., 2013; Sivaramakrishnan et al., 2009), we next focused on the consequences of chemical modulation of Ker 8 phosphorylation. To this aim, we used both the phosphatase inhibitor OA and the protein kinase activator TPA, showing a correlation with Ker 8 phosphorylation (Cadrin et al., 1992; Lee et al., 2014; Tao et al., 2016). Preliminary experiments (data not shown) evidenced that Ker 8 phosphorylation is induced by a minimum treatment-time with, respectively, OA for 2 h and TPA for 40 min at the concentrations reported in the Methods section. By temporally doubling these treatment times, no further modifications of Ker 8 nor cytotoxic effects were observed (Supplementary Table 1).

To this end, LLC-MK2 and A549 cells were either left untreated or treated with OA (for 4 h) or TPA (for 1 h and 20 min), before IIF assays to detect both Ker 8 and pKer8 (Figs. 2A-L).

The treatment with OA resulted in the clustering of pKer 8 filaments in the perinuclear area and cell rounding in both models (Figs. 2G, 2H, and 2N). This effect was rather moderate in LLC-MK2 cells but very significant in A549 cells, where the OA had induced the collapse of the pKer 8 network into dense granules, as evidenced by their strong fluorescence (see inset in Fig. 2H).

The treatment with TPA had caused the perinuclear ramming of pKer 8 (Figs. 2K and 2L), and raised the Ker 8 phosphorylation, especially in A549 cells (Fig. 2L, and 2O). In particular, the quantitative analysis (Fig. 2M) of the immunofluorescence signal associated to pKer8 in LLC-MK2 and A549 cells (Fig. 2C vs. 2K and Fig. 2D vs. 2L) well evidenced its redistribution toward the cell nuclei upon TPA treatment.

The parallel analysis of Ker 8 expression and localization after the above-mentioned treatments in both cell models (Figs. 2E, 2F, 2I, and 2J) pointed up effects that involve the entire network of Ker 8 filaments and not only its phosphorylated component.

The quantitative analyses of the immunofluorescence signal associated to Ker 8 and pKer 8 shown in the Supplementary Fig. 1 were in general consistent with the findings above reported.

In parallel, the specificity of the anti-pKer 8 antibodies was evaluated by immunoblotting assays (Supplementary Fig. 2). To this aim, the nitrocellulose membranes were either untreated or pretreated with alkaline phosphatase before incubation with anti-pKer 8 antibodies, as detailed in the Methods section. The results demonstrate the specificity of the above-mentioned antibodies, because the treatment with alkaline

phosphatase almost completely eliminated their immunoreactivity (Supplementary Fig. 2 AP pretreatment vs. untreated control).

Having observed that the drug treatments had affected pKer 8 distribution in different ways in the models studied, we were interested to discover whether and how this influences virus infection. To this end, LLC-MK2 and A549 cells were either left untreated or pre-treated with OA (for 2 h) and TPA (for 40 min) to induce IFs modifications, and then subjected to NWS/33 virus infection (MOI = 0.1 PFU/cell, 24 h) in the absence or presence of OA for 2 h p.i. and TPA for 40 min p.i. for a total treatment-time of 4 h with OA and 1 h 20 min with TPA, before IIF staining of viral NP. The results (Fig. 2P) showed that the portion of viral NP-positive cells had diminished to some extent in LLC-MK2 cells treated with OA, while in A549 cells it had slightly increased. In contrast, treatment with TPA had decreased the portion of viral NP-positive LLC-MK2 cells and increased that of A549 cells (Fig. 2P).

We next checked, using $TCID_{50}$ assays, whether the above-mentioned treatments had influenced the emergence of the viral progeny. Figure 2Q shows that the yield of the infectious virus was in general consistent with the results of the IIF assays.

We then analyzed by WB how the levels of Ker 8 and pKer 8 had been affected by treatments with the above-described drugs and virus infection (Figs. 2R-U). In LLC-MK2 cells, the treatments with OA (Fig. 2R) and TPA (Fig. 2T) slightly affected Ker 8 levels compared to the untreated cells. NWS/33 virus infection (MOI = 2 PFU/cell, 24 h) carried out in the absence or presence of OA had slightly decreased the levels of Ker 8 (Figs. 2R), which remained almost univariate in the absence or presence of TPA (Fig. 2T).

In A549 cells, the exposure to both OA and TPA had not significantly changed Ker 8 expression compared to the untreated cells (Figs. 2S and 2U). NWS/33 virus infection carried out alone or in the presence of OA and TPA had slightly increased the Ker 8 level (Figs. 2S and 2U).

PKer 8 was scarcely expressed in both models (Figs. 2R-U). In LLC-MK2 cells, no relevant changes in pKer 8 levels were seen as a result of either the drug treatments or viral infection (Fig. 2R and 2T). Conversely, in A549 cells, the levels of pKer 8 had increased after drug treatments and viral infection with more relevant effects in case of TPA treatment (Figs. 2S and 2U).

3.3. Influenza A/NWS/33 virus infection differentially modifies Ker 8 network in LLC-MK2 and A549 cells

We then analyzed the expression and phosphorylation state of Ker 8 during NWS/33 virus infection. To this end, LLC-MK2 and A549 cells were either uninfected or infected with NWS/33 virus (MOI = 2 PFU/cell, from 2 to 24 h of infection), before IIF staining carried out at different time intervals of virus infection to detect both Ker 8 and pKer 8 (Fig. 3, and Fig. 4).

At late times of NWS/33 virus infection, we observed changes in Ker 8 distribution and expression as a likely consequence of the cytopatic effect. More specifically, at 24 h p.i. we observed the collapse of the Ker 8 network around the nucleus of a large number of cells (Arrows in Figs. 3D and 3H).

In LLC-MK2 cells, the level of pKer 8 had remained almost unchanged throughout the 24 h of infection (Figs. 3J, 3K, 3L vs. 3I, and Fig. 4D vs. 4C), while in A549 cells an increase in pKer 8 level starting from 2 h p.i. (Fig. 4H vs. 4G) until 24 h p.i. was evident (Figs. 3N, 3O, and 3P vs. 3M). In parallel, NWS/33 virus infection was monitored by IIF staining of viral NP in LLC-MK2 (Figs. 3R, 3S, and 3T) and A549 (Figs. 3V, 3W, and 3X) cells. At 4 h p.i. an initial viral NP nuclear accumulation was observable in infected-LLC-MK2 cells with a mean of 46.8 ± 2.7% of the cell monolayer (Fig. 3R), while in the most part of infected-A549 cells (53.3 ± 6.2%) viral NP was present in both the cytoplasm and nucleus (Fig. 3V). The portion of viral NP present in the cytoplasm progressively increased from 8 (LLC-MK2: 63.2 ± 2.5%; A549: 78.5 ± 4.4%) to 24 h p.i. (LLC-MK2: 92 ± 2.7%; A549: 96.4 ± 3.7%) in both models, involving almost all of the cell monolayers. The intracellular distribution of viral NP in relation to either Ker 8 or pKer 8 at 24 h p.i. was assessed in the studied models by double immunostaining experiments (Fig. 4I-T).

3.4. Viral NP partially colocalizes with Ker 8 and pKer 8 during the early stages of influenza A/NWS/33 virus infection in A549 cells

In order to analyze the subcellular distribution of Ker 8 and pKer 8 in comparison with viral NP, LLC-MK2 and A549 cells were infected for, respectively, 1 h and 30 min and 1 h with NWS/33 virus (MOI = 10 PFU/cell), followed by confocal microscopy analysis (Figs. 5 and 6). The subcellular distribution of Ker 8 and viral NP evidenced a partial colocalization in A549, while in LLC-MK2 cells very weak signals of colocalization were detected (Figs. 5B2 and 5B3 vs. Figs. 5A2 and 5A3). Controls were in parallel carried out in uninfected A549 and LLC-MK2 cells. To this aim, the cells were immunostained for the detection of Ker 8 (5C and 5D) or pKer

8 (6C and 6D) in association with viral NP (5C1, 5D1, 6C1, and 6D1) in order to assess the absence of background signals in the red channel.

Moreover, faint signals of colocalization of pKer 8 with viral NP were evidenced in A549, but not in LLC-MK2 cells (Figs. 6B2 and 6B3 vs. Figs. 6A2 and 6A3).

3.5. Influenza A virus but not RSV infection enhances Ker 8 phosphorylation in human epithelial cells

In order to deepen the results previously described, we next investigated the phosphorylation level of Ker 8 in human epithelial cells inoculated with samples from the upper respiratory tract of pediatric patients with acute respiratory disease found positive for either influenza A virus or RSV, as described in the Methods section (Fig. 7). Upon 24 (Fig. 7A-B2) or 48 h p.i. (Fig. 7C-C2), A549 (Fig. 7A-A2) and HEp-2 (Fig. 7 B-C2) cell monolayers were subjected to IIF assays in order to detect pKer 8 (Fig. 7A1, B1, and C1) in comparison with influenza A virus NP (Fig. 7A) or RSV fusion protein (Fig. 7B, and C).

The results showed an increased pKer 8 level in influenza A virus-positive cells (pointed arrows in Fig. 7A1). Conversely, pKer 8 had remained almost unchanged in RSV-positive cells, also at late times of infection (circle in Fig. 7B1, and dashed circle in Fig. 7C1).

4. DISCUSSION

Influenza is one of the main public health problems worldwide (Belser et al., 2011; Ryan et al., 2018). Productive infection strictly depends on the influenza virus's ability to co-opt the biosynthetic apparatus of the host cell. We ourselves have previously assessed various cytoskeletal restriction factors against NWS/33 virus infection (Arcangeletti et al., 2008; De Conto et al., 2018, 2015, 2012, 2011).

The objective of this study was to evaluate the involvement of Ker 8 during NWS/33 virus infection in LLC-MK2 (semi-permissive) and A549 (permissive) mammalian cells in order to ascertain if this cytoskeletal component represents a restriction factor. To this end, we analyzed Ker 8 phosphorylation, which has been associated with structural reorganization of IFs (Lee et al., 2014) and keratin's ability to polymerize (Liao and Omary, 1996; Omary et al., 1998; Ridge et al., 2005; Strnad et al., 2001; Strnad et al., 2002).

Depolymerization of IFs with acrylamide (Eckert, 1985) showed more evident outcomes in LLC-MK2 than in A549 cells, where Ker 8 and its phosphorylated form showed a higher level and specific distribution. IF depolymerization during the early stages of NWS/33 virus infection had augmented the portion of viral NP, suggesting that a dynamic arrangement of IFs may favor the viral replication cycle. However, it had not resulted in a consistent increase in the titers of the viral progeny, as assessed also at very late times of infection. In agreement with previous observations (Bhattacharya et al., 2007; Kanlaya et al., 2010), it is likely that IF depolymerization fosters the biosynthetic activities required for viral replication, affecting the late phases of the infection. Nonetheless, the time frame(s) and mechanism(s) required to completely restore the IF physiological structure after acrylamide removal remain not fully understood (Arcangeletti et al., 1997). This aspect could account for the fact that partially depolymerized IFs linger on in the late stages of the infection, affecting the emergence of viral progeny. Additionally, we showed that in LLC-MK2 cells infected with avian influenza A/FPV/Ulster 73 (H7N1) virus, the IF depolymerization hinders the release of the viral progeny (Arcangeletti et al., 1997). Similarly, the occurrence of IF modifications during infection with Argentinian Mammarenavirus (Cordo and Candurra, 2003), Foot-and-mouth disease virus (Gladue et al., 2013), Dengue virus (Kanlaya et al., 2010), and Cytomegalovirus (Miller and Hertel, 2009) lead to a decreased viral replication efficiency.

NWS/33 virus had been able to induce the onset of Ker 8 structural modifications at late stages of infection. Importantly, in A549 cells, the Ker 8 dynamism had been enhanced at early stages of infection through phosphorylation (Fig. 3). Therefore, it may be assumed that in LLC-MK2 cells there are specific regulatory factors that can counteract virus-induced phosphorylation. Nonetheless, the Ker 8 phosphorylation level assessed in LLC-MK2 cells under physiological conditions was lower compared to the A549 cells.

It has been proposed that Ker 8 might be phosphorylated by protein kinases stimulated by mitogens (Omary, 2009; Omary et al., 2006). Influenza virus activates protein kinases to promote both the transport of viral ribonucleoprotein complexes and the release of viral progeny (Kujime et al., 2000; Pleschka et al., 2001). Specifically, NWS/33 virus triggers the protein kinase levels at early stages of infection (Arora and Gasse, 1998; Kunzelmann et al., 2000), easing its entry into the host cell (Root et al., 2000). Notably, protein kinase activation favors virus entry through endocytosis (Constantinescu et al., 1991; Toker, 1998). We ourselves had reported previously that NWS/33 virus entry into LLC-MK2 cells occurs mainly by macropinocytosis (De Conto et al., 2011). Therefore, increased phosphorylation levels may be relevant for NWS/33 virus entry in A549, but not in LLC-MK2 cells.

Importantly, high phosphorylation levels have been correlated with IF disassembly (Cadrin et al., 1992) and increased keratin solubility (Omary et al., 1998). In addition, phosphorylation affects the reorganization of Ker 8 in the perinuclear area (Beil et al., 2003), correlates with disease progression (Toivola et al., 2004; Zatloukal et al., 2004), and exerts regulatory effects on keratin organization and its interaction with other molecules (Coulombe and Omary, 2002). Importantly, Rotavirus and Hepatitis B and C virus infections increase Ker 8 phosphorylation (Liao et al., 1995; Shi et al., 2010; Toivola et al., 2004).

The aforesaid evidence accounts for the fact that the IF system is affected by the regulatory activity of several cellular factors and viruses can contribute to its modulation. Interestingly, human rhinovirus serotype 2 virus is able to stimulate the cleavage of Ker 8, causing IF changes which facilitate the virus egress (Seipelt et al., 2000).

In this study we found that OA, an inhibitor of protein phosphatases (Sitprija and Sitprija, 2019), had strongly affected the IF network in A549 cells in accordance with previous data (Kasahara et al., 1993; Ku et al., 2002; Strnad et al., 2002; Yatsunami et al., 1993). Contrarily, mild effects were observed in LLC-MK2 cells. These conflicting results might be related to the presence of different phosphatases levels, which are cell model-

dependent (Duchesne et al., 2003; Ingebritsen and Cohen, 1983). Moreover, treatment with TPA, a PKC activator (Castagna et al., 1982; Chen et al., 2013), had induced a stronger accumulation of pKer 8 in the perinuclear region and, in general, an increased level of pKer 8, especially in A549 cells, as reported by other Authors (Cadrin et al., 1992; Lee et al., 2014). Of note, the above-mentioned drug treatments had augmented the replicative efficiency of NWS/33 virus in A549 cells.

Although both OA and TPA were able to modulate the phosphorylated state of Ker 8, especially in A549 cells, cautious conclusions should be drawn, since such drugs could also have effects on other cellular proteins. Further studies are needed in order to better dissect the multifaceted relationship between the influenza virus and cellular phosphorylation pathways.

The obtained findings explain the complexity of the mechanisms regulating keratin phosphorylation, which involve several factors, such as epidermal growth factor, phosphatase inhibitors and B4 leukotriene (Kasahara et al., 1993; Ku and Omary, 1997; Sivaramakrishnan et al., 2009), and show a differential expression depending on the cellular model and its condition.

In A549 cells, NWS/33 virus infection had increased the pKer 8 level. Other Authors have shown increased K10 levels in A549 cells infected with avian influenza A (H9N2) virus (Yu et al., 2016), while conflicting data have revealed a reduction in K14 upon infection with papillomavirus (Bowden et al., 1992). These observations highlight the uniqueness of the interaction occurring between different viruses and specific IF components.

Lastly, the increased Ker 8 phosphorylation observed in human epithelial cells inoculated with respiratory samples from paediatric patients positive for influenza A virus, but not for RSV, supports the supposition that this is a cell- and virus-dependent mechanism.

In conclusion, this study has developed new knowledge on the role of IFs during influenza virus infection, showing that in permissive A549 cells, but not in semi-permissive LLC-MK2 cells, NWS/33 virus is able to activate Ker 8 phosphorylation, which enhances its replicative efficiency. In this regard, it has to be considered that in LLC-MK2 cells Ker 8 is poorly expressed and organized, and, therefore, does not represent a cytoskeletal restriction factor of an extent comparable to those previously detected (De Conto et al., 2018, 2015, 2012).

Overall, the use of two cell models having different permissivity for NWS/33 virus infection allowed to highlight the uniqueness of the interaction occurring between influenza virus and Ker 8 and showed how

specific cellular factors are crucial in modulating the virus's replicative efficiency. The nature of these factors and the high complex mechanisms that regulate their functions calls for further investigation.

Funding information

This work was supported by grants allocated to Flora De Conto by the University of Parma ("*Fondi di Ateneo – FIL 2016*") and by the Italian Ministry of Education, Universities and Research (MIUR) ("*Fondo per il finanziamento delle attività di base di ricerca* (*FFABR*) *– 2017*"). The funders had no role in the study design, data collection and analysis, decision to publish, or preparation of the manuscript.

Compliance with Ethical Standards

This article does not include any studies with human participants or animals performed by any of the authors. Laboratory diagnosis for respiratory infections was performed according to the medical order; consequently, there was no need to obtain informed consent. Respiratory samples were analyzed anonymously for all the assays used. The technical staff of the laboratory performed anonymization of the samples and the Authors had no access to the data prior to its anonymization.

Conflict of interest

The authors declare that they have no conflict of interest.

Acknowledgements

The Authors thank Dr. Mirko Buttrini, Dr. Clara Maccari, and Dr. Giulia Montanari for providing technical assistance during the revision of the manuscript.

References

Arcangeletti, M.C., Pinardi, F., Missorini, S., De Conto, F., Conti, G., Portincasa, P., Scherrer, K., Chezzi, C., 1997. Modification of cytoskeleton and prosome networks in relation to protein synthesis in influenza A virus-infected LLC-MK2 cells. Virus Res. 51(1), 19-34.

Arcangeletti, M.C., De Conto, F., Ferraglia, F., Pinardi, F., Gatti, R., Orlandini, G., Covan, S., Motta, F., Rodighiero, I., Dettori, G., Chezzi, C., 2008. Host-cell-dependent role of actin cytoskeleton during the replication of a human strain of influenza A virus. Arch. Virol. 153(7), 1209-1221. doi:10.1007/s00705-008-0103-0.

Arora, D.J., Gasse, N., 1998. Influenza virus hemagglutinin stimulates the protein kinase C activity of human polymorphonuclear leucocytes. Arch. Virol. 143(10), 2029-2037.

Beil, M., Micoulet, A., von Wichert, G., Paschke, S., Walther, P., Omary, M.B., Van Veldhoven, P.P., Gern, U., Wolff-Hieber, E., Eggermann, J., Waltenberger, J., Adler, G., Spatz, J., Seufferlein, T., 2003. Sphingosylphosphorylcholine regulates keratin network architecture and visco-elastic properties of human cancer cells. Nat. Cell Biol. 5(9), 803-811.

Belser, J.A., Katz, J.M., Tumpey, T.M., 2011. The ferret as a model organism to study influenza A virus infection. Dis. Model. Mech. 4(5), 575-579. doi:10.1242/dmm.007823.

Bhattacharya, B., Noad, R.J., Roy, P., 2007. Interaction between Bluetongue virus outer capsid protein VP2 and vimentin is necessary for virus egress. Virol. J. 4, 7.

Bonneau, A., Parmar, N., 2011. Double knockdown of the Rheb gene in mammalian cells using RNA interference. Biochem. Mol. Biol. The Faseb Journal. 25, Suppl 1.

Bonneau, A., Parmar, N., 2012. Effects of RhebL1 silencing on the mTOR pathway. Mol. Biol. Rep. 39(3), 2129-2137. doi:10.1007/s11033-011-0960-6.

Bowden, P.E., Woodworth, C.D., Doniger, J., DiPaolo, J.A., 1992. Down-regulation of keratin 14 gene expression after v-Ha-ras transfection of human papillomavirus-immortalized human cervical epithelial cells. Cancer Res. 52(21), 5865-5871.

Busch, T., Armacki, M., Eiseler, T., Joodi, G., Temme, C., Jansen, J., von Wichert, G., Omary, M.B., Spatz, J., Seufferlein, T., 2012. Keratin 8 phosphorylation regulates keratin reorganization and migration of epithelial tumor cells. J. Cell Sci. 125(Pt 9), 2148-2159. doi:10.1242/jcs.080127.

Cadrin, M., McFarlane-Anderson, N., Aasheim, L.H., Kawahara, H., Franks, D.J., Marceau, N., French, S.W., 1992. Differential phosphorylation of CK8 and CK18 by 12-O-tetradecanoyl-phorbol-13-acetate in primary cultures of mouse hepatocytes. Cell. Signal. 4(6), 715-722.

Castagna, M., Takai, Y., Kaibuchi, K., Sano, K., Kikkawa, U., Nishizuka, Y., 1982. Direct activation of calcium-activated, phospholipid-dependent protein kinase by tumor-promoting phorbol esters. J. Biol. Chem. 257(13), 7847-7851.

Chen, H.W., Chao, C.Y., Lin, L.L., Lu, C.Y., Liu, K.L., Lii, C.K., Li, C.C., 2013. Inhibition of matrix metalloproteinase-9 expression by docosahexaenoic acid mediated by heme oxygenase 1 in 12-O-tetradecanoylphorbol-13-acetate-induced MCF-7 human breast cancer cells. Arch. Toxicol. 87(5), 857-869. doi:10.1007/s00204-012-1003-3.

Chiou, Y.Y., Fu, S.L., Lin, W.J., Lin, C.H., 2012. Proteomics analysis of in vitro protein methylation during Src-induced transformation. Electrophoresis. 33(3), 451-461. doi: 10.1002/elps.201100280.

Constantinescu, S.N., Cernescu, C.D., Popescu, L.M., 1991. Effects of protein kinase C inhibitors on viral entry and infectivity. FEBS Lett. 2920(1-2), 31-33.

Cordo, S.M., Candurra, N.A., 2003. Intermediate filament integrity is required for Junín virus replication. Virus Res. 97(1), 47-55.

Coulombe, P.A., Omary, M.B., 2002. “Hard” and “soft” principles defining the structure, function and regulation of keratin intermediate filaments. Curr. Opin. Cell Biol. 14(1), 110-122.

De Conto, F., Covan, S., Arcangeletti, M.C., Orlandini, G., Gatti, R., Dettori, G., Chezzi, C., 2011. Differential infectious entry of human influenza A/NWS/33 virus (H1N1) in mammalian kidney cells. Virus Res. 155(1), 221-230. doi:10.1016/j.virusres.2010.10.008.

De Conto, F., Di Lonardo, E., Arcangeletti, M.C., Chezzi, C., Medici, M.C., Calderaro, A., 2012. Highly dynamic microtubules improve the effectiveness of early stages of human influenza A/NWS/33 virus infection in LLC-MK2 cells. PLoS One 7(7), e41207. doi:10.1371/journal.pone.0041207.

De Conto, F., Chezzi, C., Fazzi, A., Razin, S.V., Arcangeletti, M.C., Medici, M.C., Gatti, R., Calderaro, A., 2015. Proteasomes raise the microtubule dynamics in influenza A (H1N1) virus-infected LLC-MK2 cells. Cell. Mol. Biol. Lett. 20(5), 840-866. doi:10.1515/cmble-2015-0052.

De Conto, F., Fazzi, A., Razin, S.V., Arcangeletti, M.C., Medici, M.C., Belletti, S., Chezzi, C., Calderaro, A., 2018. Mammalian Diaphanous-related formin-1 restricts early phases of influenza A/NWS/33 virus (H1N1) infection in LLC-MK2 cells by affecting cytoskeleton dynamics. Mol. Cell. Biochem. 437(1-2), 185-201. doi:10.1007/s11010-017-3107-9.

De Conto, F., Conversano, F, Medici, MC, Ferraglia, F, Pinardi, F, Arcangeletti, MC, Chezzi, C, Calderaro, A., 2019. Epidemiology of human respiratory viruses in children with acute respiratory tract infection in a 3-year hospital-based survey in Northern Italy. Diagn. Microbiol. Infect. Dis. 94(3), 260-267. doi:10.1016/j.diagmicrobio.2019.01.008.

Duchesne, C., Charland, S., Asselin, C., Nahmias, C., Rivard, N., 2003. Negative regulation of beta-catenin signaling by tyrosine phosphatase SHP-1 in intestinal epithelial cells. J. Biol. Chem. 278(16), 14274 - 14283. doi:10.1074/jbc.M300425200.

Eckert, B.S., 1985. Alteration of intermediate filament distribution in PtK1 cells by acrylamide. Eur. J. Cell Biol. 37, 169-174.

Fois, G., Weimer, M., Busch, T., Felder, E.T., Oswald, F., von Wichert, G., Seufferlein, T., Dietl, P., Felder, E., 2013. Effects of keratin phosphorylation on the mechanical properties of keratin filaments in living cells. FASEB J. 27(4), 1322-1329. doi: 10.1096/fj.12-215632.

Gladue, D.P., O'Donnell, V., Baker-Branstetter, R., Holinka, L.G., Pacheco, J.M., Fernández Sainz, I., Lu, Z., Ambroggio, X., Rodriguez, L., Borca, M.V., 2013. Foot-and-mouth disease virus modulates cellular vimentin for virus survival. J. Virol. 87(12), 6794-6803. doi:10.1128/JVI.00448-13.

Groenewoud, M.J., Goorden, S.M., Kassies, J., Pellis-van Berkel, W., Lamb, R.F., Elgersma, Y., Zwartkruis, F.J., 2013. Mammalian target of rapamycin complex I (mTORC1) activity in ras homologue enriched in brain (Rheb)-deficient mouse embryonic fibroblasts. PLoS One 8(11), e81649. doi:10.1371/journal.pone.0081649.

Hertel, L., 2011. Herpesviruses and intermediate filaments: close encounters with the third type. Viruses 3(7), 1015-1040. doi:10.3390/v3071015.

Hyder, C.L., Pallari, H.M., Kochin, V., Eriksson, J.E., 2008. Providing cellular signposts-post-translational modifications of intermediate filaments. FEBS Lett. 582(14), 2140-2148. doi:10.1016/j.febslet.2008.04.064.

Ingebritsen, T S, Cohen, P., 1983. "Protein phosphatases: properties and role in cellular regulation." Science (New York, N.Y.) vol. 221,4608: 331-338. doi:10.1126/science.6306765.

Izawa, I., Inagaki, M., 2006. Regulatory mechanisms and functions of intermediate filaments: a study using site- and phosphorylation state-specific antibodies. Cancer Sci. 97(3), 167-174.

Kanlaya, R., Pattanakitsakul, S.N., Sinchaikul, S., Chen, S.T., Thongboonkerd, V., 2010. Vimentin interacts with heterogeneous nuclear ribonucleoproteins and dengue nonstructural protein 1 and is important for viral replication and release. Mol. Biosyst. 6(5), 795-806. doi:10.1039/b923864f.

Kasahara, K., Kartasova, T., Ren, X.Q., Ikuta, T., Chida, K., Kuroki, T., 1993. Hyperphosphorylation of keratins by treatment with okadaic acid of BALB/MK-2 mouse keratinocytes. J. Biol. Chem. 268(31), 23531-23537.

Ku, N.O., Omary, M.B., 1997. Phosphorylation of human keratin 8 in vivo at conserved head domain serine 23 and at epidermal growth factor-stimulated tail domain serine 431. J. Biol. Chem. 272(11), 7556-7564.

Ku, N.O., Azhar, S., Omary, M.B., 2002. Keratin 8 phosphorylation by p38 kinase regulates cellular keratin filament reorganization: modulation by a keratin 1-like disease causing mutation. J. Biol. Chem. 277(13), 10775-10782.

Kujime, K., Hashimoto, S., Gon, Y., Shimizu, K., Horie, T., 2000. p38 mitogen-activated protein kinase and c-jun-NH2-terminal kinase regulate RANTES production by influenza virus-infected human bronchial epithelial cells. J. Immunol. 164(6), 3222-3228.

Kunzelmann, K., Beesley, A.H., King, N.J., Karupiah, G., Young, J.A., Cook, D.I., 2000. Influenza virus inhibits amiloride-sensitive Na+ channels in respiratory epithelia. Proc. Natl. Acad. Sci. U.S.A. 97(18), 10282-10287.

Lee, E.J., Park, M.K., Kim, H.J., Kang, J.H., Kim, Y.R., Kang, G.J., Byun, H.J., Lee, C.H., 2014. 12-O-tetradecanoylphorbol-13-acetate induces keratin 8 phosphorylation and reorganization via expression of transglutaminase-2. Biomol. Ther. (Seoul). 22(2), 122-128. doi:10.4062/biomolther.2014.007.

Liao, J., Lowthert, L.A., Omary, M.B., 1995. Heat stress or rotavirus infection of human epithelial cells generates a distinct hyperphosphorylated form of keratin 8. Exp. Cell Res. 219(2), 348-357.

Liao, J., Omary, M.B., 1996. 14-3-3 proteins associate with phosphorylated simple epithelial keratins during cell cycle progression and act as a solubility cofactor. J. Cell Biol. 133(2), 345-357.

Matsuda, K., Shibata, T., Sakoda, Y., Kida, H., Kimura, T., Ochiai, K., Umemura, T., 2005. In vitro demonstration of neural transmission of avian influenza A virus. J. Gen. Virol. 86(Pt 4), 1131-1139.

Maya, R, Oren, M., 2000. Unmasking of phosphorylation-sensitive epitopes on p53 and Mdm2 by a simple Western-phosphatase procedure. Oncogene. 19(28), 3213-5. doi: 10.1038/sj.onc.1203658.

McIntosh, P.B., Laskey, P., Sullivan, K., Davy, C., Wang, Q., Jackson, D.J., Griffin, H.M., Doorbar, J., 2010. E1--E4-mediated keratin phosphorylation and ubiquitylation: a mechanism for keratin depletion in HPV16-infected epithelium. J. Cell Sci. 123(Pt 16), 2810-2822. doi: 10.1242/jcs.061978.

Miller, M.S., Hertel, L., 2009. Onset of human cytomegalovirus replication in fibroblasts requires the presence of an intact vimentin cytoskeleton. J. Virol. 83(14), 7015-7028. doi:10.1128/JVI.00398-09.

Moch, M., Herberich, G., Aach, T., Leube, R.E., Windoffer, R., 2013. Measuring the regulation of keratin filament network dynamics. Proc. Natl. Acad. Sci. U.S.A. 110(26), 10664-10669. doi:10.1073/pnas.1306020110.

Omary, M.B., Ku, N.O., Liao, J., Price, D., 1998. Keratin modifications and solubility properties in epithelial cells and in vitro. Subcell. Biochem. 31, 105-140.

Omary, M.B., Ku, N.O., Tao, G.Z., Toivola, D.M., Liao, J., 2006. "Heads and tails" of intermediate filament phosphorylation: multiple sites and functional insights. Trends Biochem. Sci. 31(7), 383-394.

Omary, M.B., 2009. "IF-pathies": a broad spectrum of intermediate filament-associated diseases. J. Clin. Invest. 119(7), 1756-1762. doi:10.1172/JCI39894.

Pleschka, S., Wolff, T., Ehrhardt, C., Hobom, G., Planz, O., Rapp, U.R., Ludwig, S., 2001. Influenza virus propagation is impaired by inhibition of the Raf/MEK/ERK signaling cascade. Nat. Cell Biol. 3(3), 301-305.

Ridge, K.M., Linz, L., Flitney, F.W., Kuczmarski, E.R., Chou, Y.H., Omary, M.B., Sznajder, J.I., Goldman, R.D., 2005. Keratin 8 phosphorylation by protein kinase C delta regulates shear stress-mediated

disassembly of keratin intermediate filaments in alveolar epithelial cells. J. Biol. Chem. 280(34), 30400-30405.

Root, C.N., Wills, E.G., McNair, L.L., Whittaker, G.R., 2000. Entry of influenza viruses into cells is inhibited by a highly specific protein kinase C inhibitor. J. Gen. Virol. 81(Pt 11), 2697-2705.

Ryan, K.A., Slack, G.S., Marriott A.C., Kane J.A., Whittaker C.J., Silman N.J., Carroll M.W., Gooch K.E., 2018. Cellular immune response to human influenza viruses differs between H1N1 and H3N2 subtypes in the ferret lung. PLoS One 13(9): e0202675. doi:10.1371/journal.pone.0202675.

Sawant, M.S., Leube, R.E., 2017. Consequences of keratin phosphorylation for cytoskeletal organization and epithelial functions. Int. Rev. Cell Mol. Biol. 330, 171-225. doi:10.1016/bs.ircmb.2016.09.005.

Seipelt, J., Liebig, H.D., Sommergruber, W., Gerner, C., Kuechler, E., 2000. 2A proteinase of human rhinovirus cleaves cytokeratin 8 in infected HeLa cells. J. Biol. Chem. 275(26), 20084- 20089. doi:10.1074/jbc.275.26.20084.

Shi, Y., Sun, S., Liu, Y., Li, J., Zhang, T., Wu, H., Chen, X., Chen, D., Zhou, Y., 2010. Keratin 18 phosphorylation as a progression marker of chronic hepatitis B. Virol. J. 7, 70. doi:10.1186/1743-422X-7-70.

Shoeman, R.L., Hüttermann, C., Hartig, R., Traub, P., 2001. Amino-terminal polypeptides of vimentin are responsible for the changes in nuclear architecture associated with human immunodeficiency virus type 1 protease activity in tissue culture cells. Mol. Biol. Cell 12(1), 143-154.

Sihag, R.K., Inagaki, M., Yamaguchi, T., Shea, T.B., Pant, H.C., 2007. Role of phosphorylation on the structural dynamics and function of types III and IV intermediate filaments. Exp. Cell Res. 313(10), 2098-2109.

Sitprija, V., Sitprija, S., 2019. Marine toxins and nephrotoxicity: mechanism of injury. Toxicon. 161, 44-49. doi:10.1016/j.toxicon.2019.02.012.

Sivaramakrishnan, S., Schneider, J.L., Sitikov, A., Goldman, R.D., Ridge, K.M., 2009. Shear stress induced reorganization of the keratin intermediate filament network requires phosphorylation by protein kinase C zeta. Mol. Biol. Cell 20(11), 2755-2765. doi:10.1091/mbc.E08-10-1028.

Snider, N.T., Omary, M.B., 2016. Assays for posttranslational modifications of intermediate filament proteins. Methods Enzymol. 568, 113-138. doi:10.1016/bs.mie.2015.09.005.

Sripada, S., Dayaraj, C., 2010. Viral interactions with intermediate filaments: paths less explored. Cell Health Cytoskelet. 2(1), 1-7.

Stefanovic, S., Windsor, M., Nagata, K.I., Inagaki, M., Wileman, T., 2005. Vimentin rearrangement during African swine fever virus infection involves retrograde transport along microtubules and phosphorylation of vimentin by calcium calmodulin kinase II. J. Virol. 79(18), 11766-11775.

Strnad, P., Windoffer, R., Leube, R.E., 2001. In vivo detection of cytokeratin filament network breakdown in cells treated with the phosphatase inhibitor okadaic acid. Cell Tissue Res. 306(2), 277-293.

Strnad, P., Windoffer, R., Leube, R.E., 2002. Induction of rapid and reversible cytokeratin filament network remodeling by inhibition of tyrosine phosphatases. J. Cell Sci. 115(Pt 21), 4133-4148.

Strober, W., 2015. Trypan Blue Exclusion Test of Cell Viability. Curr. Protoc. Immunol. 111:A3.B.1-A3.B.3. doi: 10.1002/0471142735.ima03bs111..

Tao, G.Z., Toivola, D.M., Zhou, Q., Strnad, P., Xu, B., Michie, S. A., Omary, M.B., 2006. Protein phosphatase-2A associates with and dephosphorylates keratin 8 after hyposmotic stress in a site- and cell-specific manner. Journal of cell science, 119(Pt 7), 1425–1432. https://doi.org/10.1242/jcs.02861

Toivola, D.M., Ku, N.O., Resurreccion, E.Z., Nelson, D.R., Wright, T.L., Omary, M.B., 2004. Keratin 8 and 18 hyperphosphorylation is a marker of progression of human liver disease. Hepatology 40(2), 459-466.

Toker, A., 1998. Signaling through protein kinase C. Front. Biosci. 3, D1134-1147.

Wu, W., Panté, N., 2016. Vimentin plays a role in the release of the influenza A viral genome from endosomes. Virology 497, 41-52. doi:10.1016/j.virol.2016.06.021.

Yatsunami, J., Komori, A., Ohta, T., Suganuma, M., Yuspa, S.H., Fujiki, H., 1993. Hyperphosphorylation of cytokeratin by okadaic acid class tumor promoters in primary human keratinocytes. Cancer Res. 53(5), 992-996.

Yu, G., Liang, W., Liu, J., Meng, D., Wei, L., Chai, T., Cai, Y., 2016. Proteomic analysis of differential expression of cellular proteins in response to avian H9N2 virus infection of A549 cells. Front. Microbiol. 7, 1962. doi:10.3389/fmicb.2016.01962.

Zatloukal, K., Stumptner, C., Fuchsbichler, A., Fickert, P., Lackner, C., Trauner, M., Denk, H., 2004. The keratin cytoskeleton in liver diseases. J. Pathol. 204(4), 367-376.

Zou, J., Zhou, L., Du, X.X., Ji, Y., Xu, J., Tian, J., Jiang, W., Zou, Y., Yu, S., Gan, L., Luo, M., Yang, Q., Cui, Y., Yang, W., Xia, X., Chen, M., Zhao, X., Shen, Y., Chen, P.Y., Worley, P.F., Xiao, B., 2011. Rheb1 is required for mTORC1 and myelination in postnatal brain development. Dev. Cell 20(1), 97-108. doi:10.1016/j.devcel.2010.11.020.

Figure legends

Fig. 1. IF depolymerization during A/NWS/33 virus infection in LLC-MK2 and A549 cells enhances the portion of viral NP but not the viral yields. LLC-MK2 (A, C) and A549 (B, D) cells were either left untreated (A, B) or treated with ACRYL (5 mM) (C, D) for 8 h. The cells were then subjected to IIF assays to detect Ker 8 (A-D). Images were collected with a conventional fluorescence microscope (magnification x500). (E) The graph shows the percentage of viral NP-positive LLC-MK2 and A549 cells evaluated by IIF in untreated cells (NT) and in cells pre-treated with ACRYL (5 mM) for 4 h, before inoculation with A/NWS/33 virus (MOI = 0.1 PFU/cell, 24 h) in the absence (NT) or presence (ACRYL) of the drug for 4 h p.i. The cells were then immunostained with anti-NP antibodies and the number of positive cells in relation to the total cell population was expressed as a percentage. (F) Viral yields were evaluated by $TCID_{50}$ assays in MDCK cells from supernatants of LLC-MK2 and A549 cells at, respectively, 24, 48, and 72 h p.i. Values represent the mean of two independent experiments. Error bars in graphs correspond to standard deviations. * $P < 0.05$; not statistically significant (n.s.) $P > 0.05$. (G-L) Merged images showing the overlap (orange/yellow) between viral NP (red) and Ker 8 (green) in LLC-MK2 and A549 cells evaluated by IIF. (G, H) Untreated cells and (I, L) cells pre-treated with ACRYL (5 mM) for 4 h, before inoculation with A/NWS/33 virus (MOI = 0.1 PFU/cell, 24 h) in the absence (G, H) or presence (I, L) of the drug for 4 h p.i. Scale bar = 20 μm.

Fig. 2. Ker 8 phosphorylation activation by chemical treatments enhances A/NWS/33 virus infection efficiency in A549 cells. LLC-MK2 (A, C, E, G, I, K) and A549 (B, D, F, H, J, L) cells were untreated (A-D) or treated with either OA (0.05 μg/ml) (E- H) for 4 h or TPA (LLC-MK2: 25 nM; A549: 50 nM) (I- L) for 1 h and 20 min. The cells were then subjected to IIF assays to detect Ker 8 (A, B, E, F, I, J) and pKer 8 (C, D, G, H, K, L). Images were collected using a conventional fluorescence microscope (magnification x500). Scale bar = 20 μm. (F, H) The insets show a higher magnification (x2000) of the Ker 8 and pKer 8 patterns of the cell included within the dotted area. (M, O) Quantitative analysis with the CellProfiler software of the immunofluorescence signal of pKer 8 of the images related to the TPA treatment in A549 and LLC-MK2 cells. Boundary of 10 cells per experiment were manually identified and the nuclei region was excluded. (M) To analyze the distribution of the intensity of the immunostaining of pKer 8, each cell was divided onto 8 equal

size shells. For each shell, the fraction of total staining (FractAtD) was calculated. To analyze the overall intensity of immunostaining an Integrated Intensity parameter was calculated for each cell. (N) Bar histogram related to the analysis of cell shape upon OA treatment in LLC-MK2 and A549 cells. (P) The graph shows the percentage of viral NP-positive LLC-MK2 and A549 cells evaluated by IIF in untreated cells (NT) or in cells pre-treated with OA for 2 h and TPA for 40 min, before inoculation with A/NWS/33 virus (MOI = 0.1 PFU/cell, 24 h) in the absence (NT) or presence of OA for 2 h p.i. and TPA for 40 min p.i. The cells were then immunostained with anti-NP antibodies and the number of positive cells in relation to the total cell population was expressed as a percentage. (Q) Viral yields were evaluated by $TCID_{50}$ assays in MDCK cells from supernatants of LLC-MK2 and A549 cells. Values represent the mean of two independent experiments. Error bars in graphs correspond to standard deviations. * $P < 0.05$; n.s. $P > 0.05$. (R-U) The level of Ker 8 and pKer 8 was evaluated by WB assays in uninfected (NO INF) LLC-MK2 (R, T) and A549 (S, U) cells either left untreated (cc) or treated with OA (+OA) for 4 h and TPA (+TPA) for 1 h and 20 min. In parallel, Ker 8 and pKer 8 levels were evaluated in infected (INF) LLC-MK2 (R, T) and A549 (S, U) cells either left untreated (24 h) or pre-treated with OA (24 h+OA) for 2 h and TPA (24 h+TPA) for 40 min, before inoculation with A/NWS/33 virus (MOI = 2 PFU/cell, 24 h) in the absence (24 h) or presence of OA (24 h+OA) for 2 h p.i. and TPA (24 h+TPA) for 40 min p.i. (R-U) The presence of beta-actin was checked in parallel as a protein loading control. Quantitation of protein band intensity relative to beta-actin control are shown in the bar histograms to the right of each WB assay.

Fig. 3. A/NWS/33 virus modifies Ker 8 organization in LLC-MK2 and A549 cells late in infection, while it enhances Ker 8 phosphorylation in A549 cells at early stages of its replication cycle. LLC-MK2 and A549 cells were either uninfected (A, E, I, M, Q, U) or infected with A/NWS/33 virus at an MOI of 2 PFU/cell for, respectively, 2 h (see Fig. 4), 4 h (B, F, J, N, R, V), 8 h (C, G, K, O, S, W), and 24 h (D, H, L, P, T, X). The cells were then subjected to IIF assays to detect Ker 8 (A-H), pKer 8 (I-P) and a merge (LLC-MK2: Q-T; A549: U-X) between viral NP (red) and nuclear chromatin staining with DAPI (blue). Merged images show the overlap (pink) between viral NP and nuclei. Images were collected with a conventional fluorescence microscope (magnification x500). Scale bar = 20 μm.

Fig. 4. Analysis of the effects of A/NWS/33 virus infection on the expression and phosphorylation levels of Ker 8 at 2 and 24 h p.i. in LLC-MK2 and A549 cells. LLC-MK2 and A549 cells were either uninfected (A, E, C, G) or infected with A/NWS/33 virus at an MOI of 2 PFU/cell for, respectively, 2 h (B, F, D, H) and 24 h (I-T). The cells were then subjected to IIF assays to detect Ker 8 (A, B, E, F, J, P), pKer 8 (C, D, G, H, M, S), viral NP (I, L, O, R), and a merge (K, N, Q, T). Merged images show the overlap (orange/yellow) between viral NP (red) and either Ker 8 (green) or pKer 8 (green). Images were collected with a conventional fluorescence microscope (magnification x500). Scale bar = 20 μm.

Fig. 5. At early phases of A/NWS/33 virus infection viral NP partially co-localizes with Ker 8 in A549 cells. LLC-MK2 and A549 cells were infected with A/NWS/33 virus at an MOI of 10 PFU/cell for 1 h and 30 min (A, A1, A2) and 1 h (B, B1, B2), respectively. The cells were then stained with IIF to detect Ker 8 (A, B) and viral NP (A1, B1), before confocal microscopy analysis. The colocalizing areas (orange/yellow) (A2, B2) are indicated by superposition of the two signals; no colocalizing areas have the original colors (green, Ker 8; red, viral NP). (A3, B3) scatter diagrams generated from the merged images A2 and B2, respectively, outlining the pixel-to-pixel correlation between the red and green channels. The Zeiss LSM 510 meta software was used to measure the weighted colocalization coefficients (green channel: Ch2-T1; red channel: Ch3-T2). In parallel, uninfected LLC-MK2 and A549 cells (C-D1) were stained with IIF for the detection of Ker 8 (C, D) and viral NP (C1, D1) to assess the absence of background signals in the red channel. Scale bar = 10 μm.

Fig. 6. Co-localization signals between viral NP and pKer 8 are detected at early phases of A/NWS/33 virus infection in A549 cells. LLC-MK2 and A549 cells were infected with A/NWS/33 virus at an MOI of 10 PFU/cell for 1 h and 30 min (A, A1, A2) and 1 h (B, B1, B2), respectively. The cells were then stained with IIF to detect pKer 8 (A, B) and viral NP (A1, B1), before confocal microscopy analysis. The colocalizing areas (orange/yellow) (A2, B2) are indicated by superposition of the two signals; no colocalizing areas have the original colors (green, pKer 8; red, viral NP). (A3, B3) scatter diagrams generated from the merged images A2 and B2, respectively, outlining the pixel-to-pixel correlation between the red and green channels. The Zeiss LSM 510 meta software was used to measure the weighted colocalization coefficients (green channel: Ch2-T1; red channel: Ch3-T2). In parallel, uninfected LLC-MK2 and A549 cells (C-D1) were stained with IIF to

for the detection of pKer8 (C, D) and viral NP (C1, D1) to assess the absence of background signals in the red channel. Scale bar = 10 μm.

Fig. 7. Ker 8 iperphosphorylation is a cell- and virus-dependent mechanism observable for influenza A virus infection in A549 cells but not for RSV infection in HEp-2 cells. Human respiratory secretions positive for either influenza A virus or RSV were inoculated in A549 (A-A2) and HEp-2 (B-C2) cell monolayers. At 24 (A-B2) or 48 h p.i. (C-C2) the cells were stained by IIF with anti-pKer 8 (A1, B1, C1), anti-influenza A virus NP (A) and anti-RSV fusion protein (B, C) antibodies. Images representing the results obtained from 10 samples (5 positive for influenza A virus, and 5 positive for RSV) were collected using a conventional fluorescence microscope (magnification x500). (A2, B2, C2) Merged images showing the overlap (orange/yellow) between viral NP (red) and pKer 8 (green) in A549 cells (A2) or between RSV fusion protein (red) and pKer 8 (green) in HEp-2 cells (B2, C2) evaluated by IIF. Arrows (A, A1) and circles (B, B1, C, C1) highlight infected cells. Scale bar = 20 μm.

Supplementary Fig. 1. Quantitative analysis of the immunofluorescence signal associated to Ker 8 and pKer8 upon treatment with the phosphorylation modulators OA and TPA in LLC-MK2 and A549 cells. (A-F) The IIF images related to Ker 8 and pKer 8 immunostainings in LLC-MK2 and A549 cells shown in Fig. 2A-L were analyzed with the CellProfiler software. Boundary of 10 cells per experiment were manually identified and the nuclei region was excluded. (A, C, D, F) To analyze the distribution of the intensity of the immunostainings, each cell was divided onto 8 equal size shells. For each shell, the fraction of total staining (FractAtD) was calculated. To analyze the overall intensity of immunostaining an Integrated Intensity parameter was calculated for each cell. (B, E) Bar histograms showing the analysis of the cell shape.

Supplementary Fig. 2. Analysis of phosphorylation specificity by Western blotting using alkaline phosphatase nitrocellulose membrane treatment. Cell lysates of LLC-MK2 and A549 cells were loaded onto sodium dodecyl sulphate-13% polyacrylamide gel electrophoresis and then transferred onto nitrocellulose blotting membranes. The membranes were then incubated for 30 min in phosphatase buffer, in the presence

(AP pretreatment) or absence (untreated control) of alkaline phosphatase (20 units/ml). Subsequently, WB assays were performed for the detection of pker 8 and beta-actin.

Declaration of interests

☒ The authors declare that they have no known competing financial interests or personal relationships that could have appeared to influence the work reported in this paper.

☐The authors declare the following financial interests/personal relationships which may be considered as potential competing interests: